Title
Filtering higher-order laser modes using leaky plasma channels

Journal
Physics of Plasmas, 25(1)

ISSN
1070-664X

Authors
Djordjević, BZ
Benedetti, C
Schroeder, CB
et al.

Publication Date
2018

DOI
10.1063/1.5006198

Peer reviewed

Filtering higher-order laser modes using leaky plasma channels

B. Z. Djordjević, C. Benedetti, C. B. Schroeder, E. Esarey, and W. P. Leemans

Citation: Physics of Plasmas **25**, 013103 (2018); doi: 10.1063/1.5006198
View online: https://doi.org/10.1063/1.5006198
View Table of Contents: http://aip.scitation.org/toc/php/25/1
Published by the American Institute of Physics

Filtering higher-order laser modes using leaky plasma channels

B. Z. Djordjević,[1,2] C. Benedetti,[2] C. B. Schroeder,[2] E. Esarey,[2] and W. P. Leemans[1,2]
[1]Department of Physics, University of California, Berkeley, California 94720, USA
[2]BELLA Center, Lawrence Berkeley National Laboratory, Berkeley, California 94720, USA

(Received 22 September 2017; accepted 1 December 2017; published online 2 January 2018)

Plasma structures based on leaky channels are proposed to filter higher-order laser mode content. The evolution and propagation of non-Gaussian laser pulses in leaky channels are studied, and it is shown that, for appropriate laser-plasma parameters, the higher-order laser mode content of the pulse may be removed while the fundamental mode remains well-guided. The behavior of multi-mode laser pulses is described analytically and numerically using envelope equations, including the derivation of the leakage coefficients, and compared to particle-in-cell simulations. Laser pulse propagation, with reduced higher-order mode content, improves guiding in parabolic plasma channels, enabling extended interaction lengths for laser-plasma accelerator applications. *Published by AIP Publishing.* https://doi.org/10.1063/1.5006198

I. INTRODUCTION

An understanding of the non-idealized evolution of short and intense laser pulses in a plasma is of great importance for the field of laser-plasma interactions. Various applications and areas of research for these interactions can be found in advanced laser-fusion schemes,[1] higher harmonic generation,[2] and x-ray free electron lasers.[3] Of primary interest here are laser-plasma accelerators (LPAs),[4] in which intense laser pulses have been shown experimentally to accelerate electron bunches to GeV energies.[5,6] In an LPA, a plasma wakefield is generated by the driving laser using the ponderomotive force to create charge separation. LPAs are able to produce acceleration gradients in excess of 100 GV/m, while the maximum gradient in conventional accelerators based on radio frequency cavities is on the order of 100 MV/m. It has been shown that poor laser guiding, as a result of the presence of higher-order laser modes, can have an adverse effect on an LPA.[5]

Laser pulse propagation is optimized when the pulse enters the gas-filled discharge channel with a flat phase front. Under such conditions, we can achieve what is called "matched" guiding, in which the laser spot size remains constant ($r_s = r_0$, where r_0 is the initial spot size), e.g., a Gaussian pulse injected into a properly shaped parabolic channel. The critical channel depth for matched guiding is given by $\Delta n_c = (\pi r_e r_0^2)^{-1}$ or $\Delta n_c(\mathrm{cm}^{-3}) \approx 1.13 \times 10^{20}/r_0^2(\mu\mathrm{m})$, where $r_e = e^2/m_e c^2$ is the classical electron radius, e and m_e are the electron charge and rest mass, and c is the speed of light. The production of high quality beams from LPAs requires the laser pulse to maintain a high, constant intensity over multiple Rayleigh ranges, where the Rayleigh range is $Z_R = \pi r_0^2/\lambda$ and λ is the wavelength of the laser pulse. However, guiding can be compromised in several ways. Channel characteristics (e.g., the channel radius, density) may not be optimally matched to the pulse at focus, leading to mismatched pulse propagation, i.e., poor guiding. Likewise, realistic pulses,[5,6] which are often super-Gaussian in the transverse direction in the near field after amplification, tend to develop Bessel-like sidelobes at focus, which do not guide according to the intended Gaussian description. Oscillations due to mismatching and non-Gaussian pulse profiles can be deleterious to LPA applications, leading to non-optimal acceleration or electron bunch loss. The decrease in laser amplitude induces a reduction of the wakefield size and the bunch finds itself in the defocusing phase of the wake. In addition to mismatching, the higher-order modes leak out more readily from guiding structures, which can cause damage to the structure, notably in the case of discharge capillaries.

Guiding of a non-Gaussian pulse in a parabolic channel is challenging. One possible solution is to use a complicated plasma channel structure that is better matched to the pulse. Theoretically, in the low-intensity, low-power regime, one can guide a pulse using a transverse density profile of the form

$$\frac{n(r)}{n_0} \approx \frac{1}{k_{p0}^2}\left(\frac{\nabla_\perp^2 a_\perp(r)}{a_\perp(r)} + 1\right), \tag{1}$$

where n_0 is the on axis density of the plasma channel, $a_\perp(r) = eA_\perp(r)/m_e c^2$ is the normalized transverse component of the laser field vector potential, and $k_{p0} = \omega_{p0}/c$, where $\omega_{p0}^2 = 4\pi n_0 e^2/m_e$ is the plasma frequency.[7] Equation (1) is derived from the steady state form of the paraxial wave equation, as discussed below. An analogous tailoring of the radial profile of the refractive index in fiber optics has been used to guide an Airy-type pulse, but at much lower laser intensities than that required in LPA experiments.[8] Complicated pulse or channel profiles do not readily give solutions that are experimentally tenable. Experimentally, a ceramic aperture has been used to filter out sidelobes in the far-field.[9] While this is quite feasible, a significant amount of energy is lost in the main-lobe, a few to tens of percent, and the main-lobe still remains somewhat non-Gaussian. The solution proposed in this paper is to use a leaky channel to guide the primary Gaussian mode and to leak out the disruptive higher-order modes.

Tailored plasma structures for the purpose of controlling the evolution of laser pulses are well established,[4] notably those of parabolic and leaky channels. Leaky channels may

be made using the hydrodynamic shock (hydroshock) technique or clustered gas jets.[10–12] In both techniques, an axicon-formed pump laser is used to ionize a stream of gas and a channel is formed after several nanoseconds of evolution that is approximately parabolic near the axis of propagation and sharply truncated after several pulse-widths. Leaky channels have been previously studied for a variety of applications, such as the minimization of instabilities (e.g., forward Raman scattering).[13] The approach used in our study draws on the source dependent expansion (SDE) formalism,[14–17] which has been shown to effectively model the evolution of Laguerre-Gaussian (LG) modes, as well as the Wentzel-Kramers-Brillouin (WKB) approximation[18,19] to evaluate mode leakage in the channel.

This paper is organized as follows: in Sec. II, we discuss the general behavior and consequences of multimode laser pulses in a plasma channel. We are interested in pulses that have a jinc-type transverse profile, as well as pulses composed of Laguerre-Gaussian modes similar in profile to a jinc. In Sec. III, we model the effects of leaky channels using the WKB theory. In Sec. IV, we present the paraxial solution to the wave equation and its decomposition into LG modes via the SDE. Using particle-in-cell (PIC) simulations, in Sec. V, it is shown that the inclusion of a leakage rate coefficient in the SDE accurately models the secular evolution of the laser pulse which is in agreement with PIC simulations. Also, we provide numerical examples of sharply truncated as well as exponentially decaying leaky channels in the quasi-linear regime to further corroborate the concept. A summary and conclusion are presented in Sec. VI. Throughout this paper, we use the PIC code INF&RNO[20,21] to simulate LPA systems in 2 D, axisymmetric geometry.

II. NON-GAUSSIAN TRANSVERSE PULSE PROFILES AND PLASMA GUIDING STRUCTURES

When treated theoretically, laser pulses are generally modeled as having Gaussian profiles in the transverse direction, $a_\perp(r) = a_0 \exp(-r^2/r_0^2)$, where a_0 is the initial, on-axis laser amplitude for a Gaussian pulse, but this is not a realistic description of an experimental pulse. For example, if the laser profile at the surface of a focusing optic is a flat top, then at focus the laser profile can be better approximated by a jinc profile than a Gaussian, i.e., $\mathrm{jinc}(r) = 2J_1(\kappa r/r_0)/(\kappa r/r_0)$, where $J_1(r)$ is the first order Bessel function of the first kind and $\kappa = 2.74331$ is a scale parameter so that the jinc profile has the same Full-Width Half-Maximum (FWHM) as the Gaussian pulse. For analytical tractability, we can decompose a jinc pulse into Laguerre-Gaussian (LG) modes, $L_m(2r^2/r_{\mathrm{LG}}^2)\exp(-r^2/r_{\mathrm{LG}}^2)$, where the Laguerre polynomials $L_m(x) = \frac{1}{m!}(\frac{d}{dx} - 1)^m x^m$ is the Laguerre polynomial of order m and the first three polynomials are $L_0(x) = 1$, $L_1(x) = 1 - x$, and $L_2(x) = 1 - 2x + \frac{1}{2}x^2$, and $r_{\mathrm{LG}} = 1.144 r_0$ for three modes when matching the FWHM of the superposition of the three modes to a Gaussian as well as a jinc profile. Note, in this instance, since $r_{\mathrm{LG}} \neq r_0$, each individual LG mode is inherently mismatched if the channel depth is chosen to be matched for the Gaussian. Theoretically, it would simplify the problem to pick $r_{\mathrm{LG}} = r_0$ for the LG decomposition; however, this decomposition choice reflects the experimental practice of defining the pulse by the FWHM of the main-lobe regardless of modal content (which is not the correct pulse-width to which we should match a parabolic channel for guiding). For simplicity, only azimuthally symmetric modes are considered. In our simulations we use three LG modes (LG3) because, up to a radius of 250 μm, a typical radius for a capillary channel used for guiding, three appropriately matched LG modes accurately model the main lobe and first sidelobe of a jinc pulse, while accounting for 94% of the power content. The initial values of the LG decomposition are chosen by using a nonlinear fit to match the peak, the FWHM of the main lobe, and the first zero of the jinc pulse. Gaussian, jinc, and LG3 pulse profiles are shown in Fig. 1. The presence of sidelobes in a jinc profile, or higher-order modes in an LG decomposition, can be shown to lead to mode beating that causes significant oscillations in the pulse intensity and poor guiding.

As a demonstration of the behavior of realistic pulse propagation, we compare the evolution of a Gaussian, jinc, and LG3 pulse in a matched parabolic channel, given by the following equation:

$$n(r) = n_0\left[1 + \frac{4}{(k_{p0}R)^2}\frac{r^2}{r_0^2}\right], \tag{2}$$

where R is the characteristic radius of the channel, and for matched propagation $R = r_0$. In Fig. 2 it is demonstrated that, where an ideal Gaussian pulse with a Rayleigh length of $Z_R = 1.083$ cm would be guided, the presence of sidelobes causes the pulse to suffer from significant beating between the modes. Even though individual LG modes are guided by a parabolic channel, the superposition of multiple modes causes beating of the form $\approx 2a_m(z)a_n(z)\cos[\phi_m(z) - \phi_n(z)]$,[22] where a_m and ϕ_m are the amplitude and phase, respectively, of the corresponding LG mode. For linearly polarized LG modes, one has $\phi_m - \phi_n = k_{\mathrm{beat}}z$, where $k_{\mathrm{beat}} = 2(m-n)/Z_R$.

In order to offset the negative influences of sidelobes, we propose the use of plasma structures such as leaky channels. The application of plasma lenses and filters can compensate for the constraints of the optical systems,[23,24] providing additional pulse tuning after amplification or compression. In this paper, we investigate the effects of plasma structures, more specifically leaky channels, on multimode

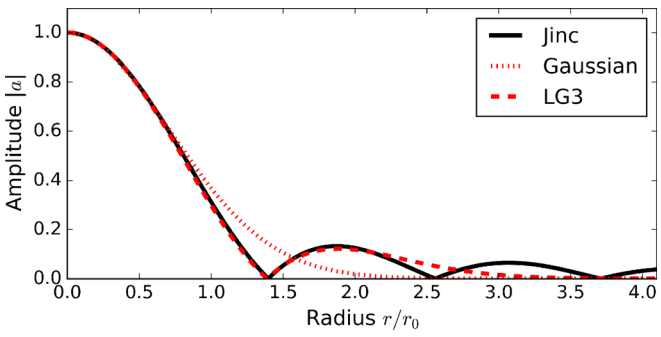

FIG. 1. Comparison of a Gaussian pulse with $r_0 = 53$ μm, a jinc-type profile, and a superposition of three LG modes. For the jinc profile, $\kappa = 2.74331$ and for the LG3 profile, $\sum_{m=1}^{3} a_m L_m(2r^2/r_{\mathrm{LG}}^2)\exp(-r^2/r_{\mathrm{LG}}^2)$, where the mode amplitudes are $a_0 = 0.729$, $a_1 = 0.418$, and $a_2 = -0.146$ and the LG3 matched radius is $r_{\mathrm{LG}} = 1.144 r_0$.

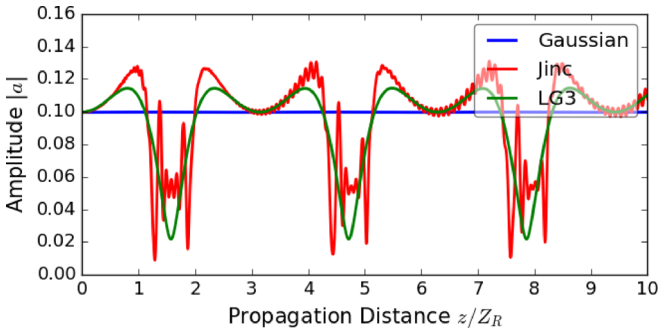

FIG. 2. Evolution of the normalized laser amplitude a for a non-Gaussian pulse in a parabolic channel with $R = r_0$. The blue line corresponds to a for a Gaussian pulse, the red line to a jinc pulse, and the green line to an LG3 pulse, i.e., $\sum_{m=1}^{3} a_m L_m(2r^2/r_{\mathrm{LG}}^2)\exp(-r^2/r_{\mathrm{LG}}^2)$. The simulation parameters are $r_{\mathrm{LG}} = 1.144r_0$, $r_0 = 53$ μm, and $Z_R = 1.083$ cm, initial amplitude $a_\perp(0) = 0.1$, $n_0 = 10^{17}$ cm^{-3}, mode amplitudes $a_0 = 0.729$, $a_1 = 0.418$, and $a_2 = -0.146$, an LG3 matched radius of $1.144r_0$, and a jinc matching parameter of $\kappa = 2.74331$. (Pulse profiles shown in Fig. 1.).

laser pulses for the purpose of improving laser guiding and evolution. In our analytic formulation, we assume the low intensity limit $a \ll 1$, which neglects nonlinear effects such as self-focusing and wakefield generation. These results are compared to fully nonlinear simulations for cases where $a \approx 1$.

We generally focus on sharp truncations in the plasma density profile as seen in Fig. 3 (solid blue curve), analytically expressible by multiplying the density profile by a Heaviside function $\Theta(r_{\mathrm{cut}} - r)$, where r_{cut} is the truncation radius of the channel. Also analytically tractable are leaky channels with linearly or exponentially decaying density gradients, where we multiply the density function $n(r)$ by the factor $\exp(-r^2/r_{\mathrm{ED}}^2)$ (dotted and dashed-dotted curves), where r_{ED} is a constant and the effective channel radius near the axis is

$$R_{\mathrm{eff}} = R\left[1 - \left(\frac{k_{p0}r_0R}{2r_{\mathrm{ED}}}\right)^2\right]^{-1/2}. \tag{3}$$

III. WKB METHOD

A general treatment of the power loss from the leaky plasma channel can be achieved via the WKB method. Heuristically, we do this by assuming first that modal power loss is given by[25]

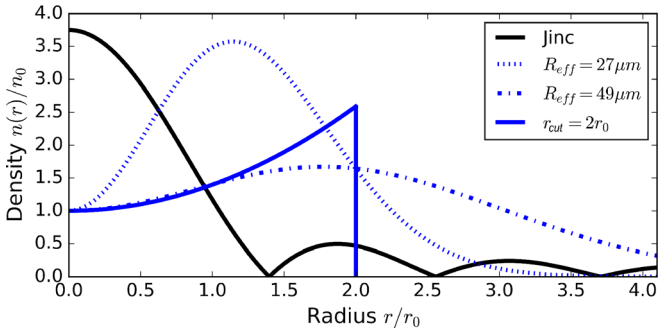

FIG. 3. Examples of theoretical models used in simulating truncated plasma channels relative to a Gaussian pulse with $r_0 = 53\,\mu$m: sharp truncation at $r_{\mathrm{cut}} = 2r_0$ (solid curve), exponentially decaying walls with a matched effective radius, i.e., $R_{\mathrm{eff}} \approx r_0$ (dash-dotted curve), and exponentially decaying walls with a mismatched effective radius (dotted curve).

$$dP_m = -\hat{\gamma}_m P_m dz, \tag{4}$$

where P_m is the modal power contribution, $\hat{\gamma}_m = T_m/Z_m$, where T_m is the transverse leakage (tunneling) rate per mode m and Z_m is the characteristic propagation distance. In the case where $\hat{\gamma}_m$ does not depend on the propagation distance z, we can write

$$P_m(z) = P_m(0)\exp[-\hat{\gamma}_m z]. \tag{5}$$

In order to calculate Z_m and T_m, we use the WKB formalism.[26] Given a wave equation of the form

$$\left[\nabla_\perp^2 + K^2(r)\right]\Psi(r) = 0, \tag{6}$$

where $K^2(r) \approx \omega^2/c^2 - k_p^2(r) - k_z^2$ is the general leaky channel wavenumber, $\omega = kc = 2\pi c/\lambda$ is the frequency of the laser, $k_p^2(r) = k_{p0}^2\frac{n(r)}{n_0}$ is the wavenumber corresponding to plasma oscillations, $k_z \approx \omega^2/c^2 - k_{p0}^2 - 4(2m+1)/r_0^2$ is the axial wavenumber, and $\Psi(r)$ is a generalized potential field. For the Helmholtz equation (6), we can write down the WKB solution for an arbitrary density profile

$$\Psi(r) = \frac{C}{\sqrt{K(r)}}\exp\left[i\int^r |K(r')|dr'\right], \tag{7}$$

where C is a coefficient to be determined and the integration takes place between the turning points of K^2.

In the WKB formulation, we can describe the transverse profile with respect to incident (i), reflected (r), and transmitted (t) local plane waves, which are, respectively, distinguished by different coefficients C_i, C_r, and C_t, as well as integration limits: $r < r_{\mathrm{tp}}$ for the incident/reflected waves, where r_{tp} is a turning point for $|K|^2 = 0$ and $r > r_{\mathrm{cut}}$ for the transmitted waves. In the region $r_{\mathrm{tp}} < r < r_{\mathrm{cut}}$, the field is evanescent and decreases exponentially with r, which in turn is characterized by C_e.

Using the standard connection formulas for the WKB theory, by which we can write $C_i = C_e, C_t = C_e\exp[-\int_{r_{\mathrm{tp}}}^{r_{\mathrm{cut}}}|K|dr]$, the transmission coefficient[25] for the transverse laser profile is

$$T = \frac{|\Psi_t|^2}{|\Psi_i|^2} = \frac{|C_t|^2}{|C_i|^2} = \exp\left[-2\int_{r_{\mathrm{tp}}}^{r_{\mathrm{cut}}}|K|dr\right], \tag{8}$$

and the propagation distance between turning points along a ray path is

$$Z_m = 2k_z\int_0^{r_{\mathrm{tp}}}|K|^{-1}dr \approx \pi Z_R. \tag{9}$$

While T_m is an accurate calculation of the leakage rate, it neglects the effect of multi-mode interference, which is not explored in this paper but has been explored in other fields.[27]

For the m-th order LG mode propagating in a sharply truncated parabolic channel, the leakage rate is defined as[12]

$$T_m = \left[\frac{r_{\mathrm{cut}}}{\mu R} + \left(\frac{r_{\mathrm{cut}}^2}{(\mu R)^2} - 1\right)^{1/2}\right]^{2\mu^2} \times \exp\left[-2\mu\frac{r_{\mathrm{cut}}}{r_0}\left(\frac{r_{\mathrm{cut}}^2}{(\mu R)^2} - 1\right)^{1/2}\right], \tag{10}$$

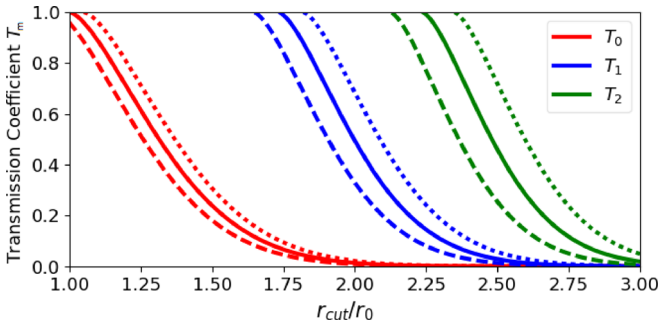

FIG. 4. Leakage coefficients (T_m) estimated with the WKB theory for the first three modes ($m=0$—red, $m=1$—blue, and $m=2$—green) for varying channel radii ($R/r_0 = 0.95$—dashed, 1.0—solid, and 1.05—dotted).

where $\mu = \sqrt{2m+1}$. Figure 4 shows T_m for modes $m=0$, 1, and 2, and channel radii $R/r_0 = 0.95, 1.0, 1.05$. Higher-order modes leak out at a much faster rate than the fundamental for all cutoff radii and higher-order modes are more sensitive to deviations in the characteristic guiding radius of the channel. Likewise, all leakage coefficients saturate to a value of one below a certain cutoff radius, i.e., the vacuum diffraction rate. The channel parameters can be chosen using Fig. 5, where the white line governs the maximum leakage coefficient T_1 for the $m=1$ LG mode for varying channel parameters. Higher-order modes will have a shallower slope since they will leak out even faster. Wider truncation radii allow for a lower T_0/T_1 ratio but slower overall leakage.

IV. SOURCE DEPENDENT EXPANSION

A useful way to describe pulse propagation in an infinite parabolic channel is the SDE.[14,15] Below, we will extend the SDE to truncated channels by incorporating our results from the WKB approximation. The full wave equation for the transverse vector potential is

$$\nabla^2 \mathrm{A}_\perp - \frac{1}{c^2}\frac{\partial^2 \mathrm{A}_\perp}{\partial t^2} = -\mu_0 \mathrm{J} + \frac{1}{c}\frac{\partial \nabla \Phi}{\partial t}, \tag{11}$$

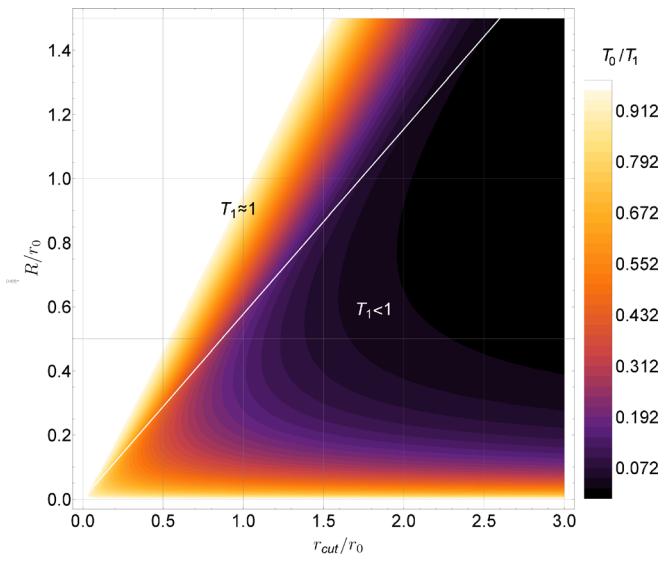

FIG. 5. Leakage coefficient ratio T_0/T_1 for varying r_{cut}/r_0 and R/r_0.

where J is the source current and Φ is the scalar potential of the laser field. In Eq. (11), we proceed to neglect the scalar potential contribution, since it is generally small within the laser pulse,[28] and we write the vector potential in the following form:

$$\mathrm{A}_\perp(r,z,t) = \hat{\mathrm{A}}(r,z,t)\exp\left[i(kz-\omega t)\right], \tag{12}$$

where $\hat{\mathrm{A}}$ is the amplitude and k and ω are the wavenumber and frequency of the laser pulse. After inserting (12) into (11), and making the slowly-varying envelope assumption $|k\frac{\partial \hat{\mathrm{A}}}{\partial z}| \gg |\frac{\partial^2 \hat{\mathrm{A}}}{\partial z^2}|$, we obtain the paraxial equation

$$\nabla_\perp^2 \hat{\mathrm{A}} + 2ik\frac{\partial \hat{\mathrm{A}}}{\partial z} = -\mu_0 \hat{\mathrm{J}}, \tag{13}$$

where $\nabla_\perp^2 = (1/r)\partial_r(r\partial_r)$ in polar coordinates and $\hat{\mathrm{J}}$ is the fast part of the source current.

In the SDE, where we work with the normalized vector potential $\hat{a} = e\hat{\mathrm{A}}/m_e c^2$, we are only considering the transverse field. We parameterize the pulse as $\hat{a}(r,z) = \sum_m \hat{a}_m(z) L_m[2r^2/r_s^2(z)]\exp\left\{-[1-i\alpha(z)]r^2/r_s^2\right\}$, where $\hat{a}_m(z) = C_m(z)\exp\left[i\phi_m(z)\right]$, $r_s(z)$ is the pulse spot size, $\alpha(z)$ is the inverse radius of curvature, $C_m(z)$ and $\phi_m(z)$ are the mode-specific amplitude contribution and phase. For this problem, in the axisymmetric case, we are solving the reduced wave equation, i.e., the paraxial equation

$$\left[\frac{1}{r}\frac{\partial}{\partial r}\left(r\frac{\partial}{\partial r}\right) + 2ik\frac{\partial}{\partial z}\right]\hat{a}(r,z) = -j(r,z). \tag{14}$$

In order to account for the truncated plasma channel, we may consider the source function as truncated itself, $j(r,z) = j(\xi,z) = k_{p0}^2 \frac{n(\xi)}{\gamma n_0}\Theta(\xi_{\mathrm{cut}}-\xi)a(\xi,z)$, where $\gamma = \sqrt{1+a^2} \approx 1$ since we are only considering low-power laser pulses in this paper, $\xi = 2r^2/r_s^2$, and ξ_{cut} corresponds to the truncation radius r_{cut}. This in theory will give an exact description of the laser pulse evolution, however, only if a sufficient number of modes are included.

The SDE method is well suited to describe the propagation and evolution of near-Gaussian pulses, since only a few LG modes are needed in the SDE expansion. This is the case for an idealized (infinite) parabolic channel. For a leaky channel, the SDE method becomes problematic, since a significant portion of the laser power can exist outside the channel, resulting in laser profiles consisting of a near-Gaussian core superimposed on a low amplitude radial quasi-plateau that extends to large radii and represents the leaked power outside the channel. In order to describe the low amplitude wings of the leaked laser field, the SDE method would require the retention of hundreds of LG modes.

Alternatively, to describe laser power loss in a leaky channel, we can modify the SDE equations by heuristically including a power loss damping coefficient, as determined from the above WKB theory, in the wave operator of the paraxial wave equation. Based on comparisons to simulations of the full Maxwell-plasma equations, it is found that by including this damping term, pulse evolution in a leaky channel can be modeled with the modified SDE equations using only a small number of LG modes.

In this approach, we equate the power for the LG modes, which conserve energy over all space, to a separate solution with an exponentially decaying component, that is $\hat{a}_m(z)^2 \approx a_m(z)^2 \exp(-\hat{\gamma}_m z)$, or

$$\hat{a}_m(z) \approx a_m(z) \exp(-\hat{\gamma}_m z/2), \tag{15}$$

and insert this into Eq. (14), giving us an additional term in the paraxial wave equation proportional to $\hat{\gamma}_m a$. In this case, the source term is that of the infinite channel, i.e., no Heaviside function, and for which the LG modes are the proper eigenfunctions.

In the low-power limit $a \ll 1$, analytical solutions can be derived for pulse decompositions of a few lower-order modes. Integrating the paraxial Equation (14) with respect to ξ, gives a series of decoupled equations for each of the LG modes by using the orthogonality property of the Laguerre polynomials. For the m-th radial mode

$$(\partial_z + \gamma_m + A_m)a_m - imBa_{m-1} - i(m+1)B^* a_{m+1} = -iF_m, \tag{16}$$

where $\gamma_m = \hat{\gamma}_m/2$,

$$A_m(z) = \frac{r_s'}{r_s} + i(2m+1)\left[\frac{(1+\alpha^2)}{kr_s^2} - \alpha\frac{r_s'}{r_s} + \frac{\alpha'}{2}\right],$$
$$B(z) = -\alpha\frac{r_s'}{r_s} - \frac{(1-\alpha^2)}{kr_s^2} + \alpha'/2 - i\left(\frac{r_s'}{r_s} - 2\frac{\alpha}{kr_s^2}\right),$$

where the prime $'$ corresponds to the derivative with respect to z, and

$$F_m(z) = -\frac{1}{2k}\int_0^\infty j(\xi)L_m[\xi]\exp\left[-(1+i\alpha)\xi/2\right]d\xi.$$

For three modes, assuming $|a_m| \ll 1$ for $m \geq 3$, there are four separate equations

$$\begin{aligned}(\partial_z + \gamma_0 + A_0)a_0 - iB^* a_1 &= -iF_0,\\ (\partial_z + \gamma_1 + A_1)a_1 - iBa_0 - 2iB^* a_2 &= -iF_1,\\ (\partial_z + \gamma_2 + A_2)a_2 - 2iBa_1 &= -iF_2,\\ -3iBa_2 &= -iF_3.\end{aligned} \tag{17}$$

The first three equations govern the evolution of the amplitude coefficients and phases. Using the relative smallness of the highest order terms, we obtained a fourth equation to provide closure for an initially over-determined three mode system and effectively describe the evolution of r_s and α.

The SDE is a powerful tool which allows for rapid modeling and assessment of LG laser modes in a parabolic channel. However, in order to get a more full description of laser pulse evolution, it is necessary to turn to numerical techniques, as described in Sec. V.

V. NUMERICAL RESULTS

In this section, we compare our analytic approximations with numerical analyses of multimode LG pulses propagating through leaky plasma channels. This includes comparing numerical results of the SDE equations to results from the particle-in-cell (PIC) code INF&RNO.[20,21] Of particular interest is whether the LG decomposition is sufficient to describe a jinc pulse in a leaky channel. As seen in Fig. 6, which shows results from the PIC code INF&RNO, there is a close correlation between the two even when only using an LG3 pulse. In this case, we are propagating the jinc and LG3 pulses through a leaky channel with an on axis density of $n_0 = 10^{17}$ cm^3 and a truncation radius of $r_{\text{cut}} = 2r_0$, where $r_0 = 53$ μm and the jinc matching parameter is $\kappa = 2.74331$. The numerical parameters used in the following simulations are propagation step size $k_{p0}\Delta z = 1$, plasma grid $k_{p0}\Delta r_{\text{plasma}} = 1/10$ and $k_{p0}\Delta\zeta_{\text{plasma}} = 1/20$ (where $\zeta = z - ct$ is the comoving coordinate of the pulse), and laser grid $k_{p0}\Delta r_{\text{laser}} = 1/20$ and $k_{p0}\Delta\zeta_{\text{laser}} = 1/15$. In the simulations we take $r_{\text{LG}} = r_0$ so that individual modes are matched to the channel. The parabolic profile is characterized by $R = r_0$. In this simulation, we chose to match the jinc and LG3 pulse with respect to the on-axis amplitude a, therefore, the main difference between the two is that the jinc has more energy overall so, as the fundamental evolves, it also effectively extracts energy from the higher-order modes. Otherwise, the pulse evolutions are similar.

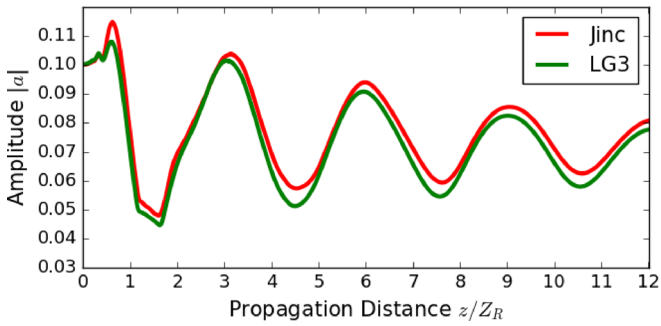

FIG. 6. PIC modeling results comparing the evolution of a jinc pulse with $\kappa = 2.74331$ and $r_0 = 53$ μm in a matched, truncated parabolic channel with $r_{\text{cut}} = 2r_0$, $Z_R = 1.083$ cm, and $n_0 = 10^{17}$ cm^{-3}, to three LG modes of amplitude $a_0 = 0.729$, $a_1 = 0.418$, and $a_2 = -0.146$, for which we normalize the initial sum such that $a_\perp(0) = 0.1$.

In Fig. 7, we can see the relative effectiveness of the SDE formulation, in which we are solving the system of Eqs. (17), relative to the PIC simulations. In this figure, we are comparing the SDE and PIC results for three different cutoff radii: (a) $r_{\text{cut}} = 3r_0$, (b) $r_{\text{cut}} = 2.25r_0$, and (c) $r_{\text{cut}} = 1.75r_0$. This is for a sharply truncated parabolic channel with $n_0 = 10^{17}$ cm^{-3} and $R = r_0$. In addition, we use an exponentially decaying numerical filter near the boundaries of the simulation to gently eliminate radiation leaked from the channel before it can be numerically reflected back into the channel. The threshold for relativistic self-focusing of a linearly polarized Gaussian laser pulse is given by the relation $P/P_{cr} = (k_{p0}r_0a_0)^2/32$, and a system is generally only significantly affected by self-focusing when $P/P_{cr} > 1$. In this case for $a \leq 0.3$ and $r_0 = 53$ μm as seen in Fig. 7, $P/P_{cr} \leq 0.06$, so self-focusing is not an important contribution to pulse evolution. It is evident that, as the cutoff radius decreases, the SDE is less able to model the evolution of the pulse in a leaky channel. However, the greatest discrepancy is near pulse injection and, as the pulse propagates, the

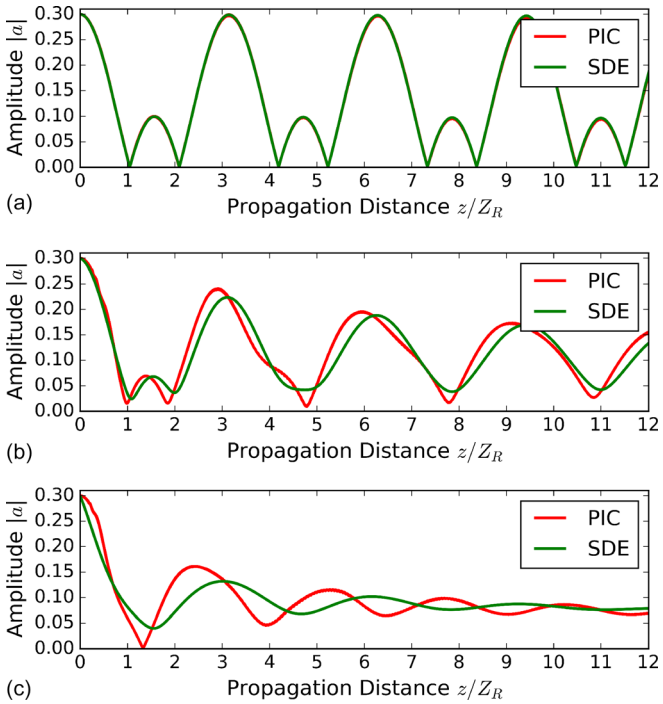

FIG. 7. Comparison of numerical PIC results with the SDE including transverse transmission coefficients calculated via the WKB theory. Three injected modes with equal initial amplitudes $a_0 = a_1 = a_2 = 0.1$, with a pulse radius of $r_0 = 53\,\mu$m and a matched parabolic density profile $R = r_0$, $Z_R = 1.083$ cm, with cutoff radii of (a) $r_{cut} = 3.0r_0$, (b) $r_{cut} = 2.25r_0$, and (c) $r_{cut} = 1.75r_0$. The WKB transmission coefficients provide accurate models of the pulse evolution for $r_{cut} > 2r_0$, but for the $r_{cut} < 2r_0$ mode, excitation leads to a discrepancy.

higher-order modes leak out faster and the SDE and PIC begin to agree again as the evolution of the fundamental mode begins to dominate. We believe that the discrepancy at the beginning of pulse evolution, most noticeable in Fig. 7(c), to be due to the coupled excitation of different modes due to back reflection from the sharp truncation, which is not accounted for in our model.

Numerical simulations show that as the pulse stabilizes, the contribution of the fundamental mode ($m = 0$) dominates and higher-order mode content leaks out and/or changes phase. This can be seen in Fig. 8, where a sharply truncated parabolic channel is used to filter a jinc pulse. Using the same numerical parameters as before, here, we have a filter that is 16 cm = 14.8 Z_R in length with a 0.5 cm gap before the pulse is injected into an "infinite" parabolic channel ($r_{cut} = 8r_0$). The purpose of this gap is to facilitate injection of the filtered pulse into the parabolic capillary discharge channel with a flatter phase front assisted by simple vacuum diffraction. In Fig. 8(a), we plot the normalized amplitude a in red while comparing it to an identical pulse injected only into an infinite parabolic channel. We can see once again how the jinc pulse will undergo much more severe oscillations if the sidelobes are not removed. The energy content of the pulse is plotted in blue and falls to about 75%. This is a significant loss, however, the Gaussian mode accounts for 68% of the initial pulse. We are mainly losing energy from the higher-order modes as shown in Fig. 8(b).

In Fig. 8(b), we show a modal decomposition of the pulse during filtering, focusing primarily on $m = 0$, 1, and 2, and can see how the higher-order modes leak out, leaving what is effectively just the 0-th and 1st order modes. We can extract the individual mode content numerically by exploiting the orthogonality property of the LG modes

$$a_m(z) = \int_0^\infty a_{tot}(z,\xi) L_m(\xi) \exp(-\xi) d\xi,$$

where $a_m(z)$ is the individual mode amplitude coefficient and the sum over a_{tot} is the total, numerical transverse lineout of the PIC-generated pulse at peak field intensity.

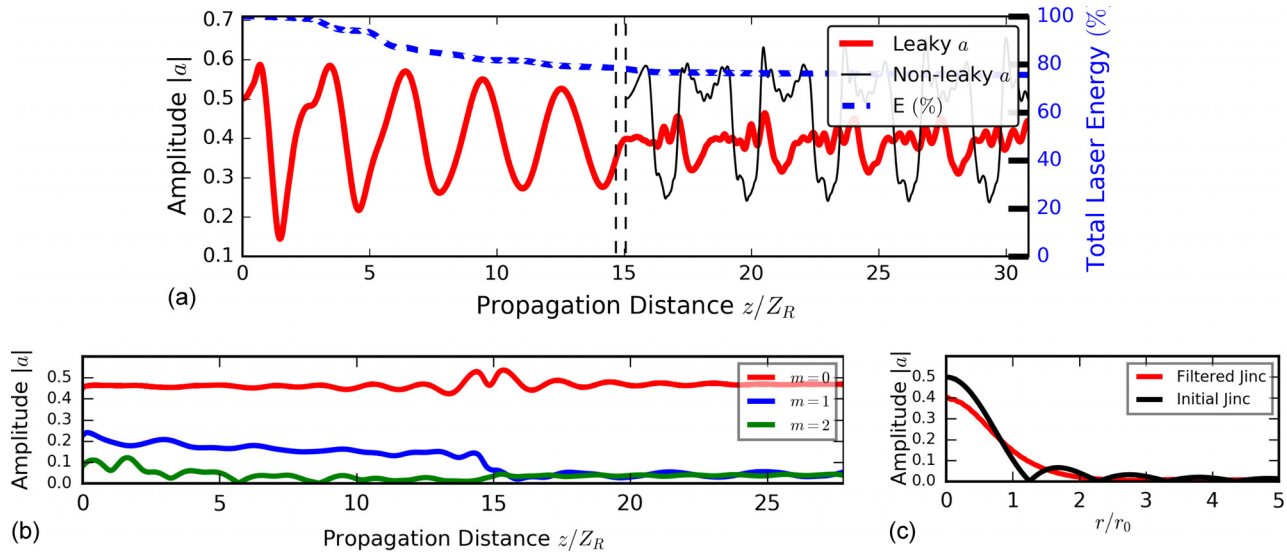

FIG. 8. A truncated leaky channel ($r_{cut} = 2.25r_0$, $n_{filter} = 10^{17}$ cm^{-3}, and length of 16 cm), acting as a filter, precedes a parabolic capillary discharge channel with $n_0 = 3 \times 10^{17}$ cm^{-3} and $R = 1.1r_0$ μm separated by a 0.5 cm gap. (a) The laser amplitude propagating through the filter into a parabolic channel is in red, an unfiltered jinc pulse propagating just through a matched infinite channel (black), and the energy content of the filtered pulse (blue). (b) Modal decomposition of intensity. The color lines represent the fundamental (red), 1st (blue), and 2nd (green) higher-order modes on the basis of an LG decomposition. (c) The initial, unfiltered pulse profile (red) and the filtered pulse profile (black), where $a_\perp(0) = 0.5$, $r_0 = 53\,\mu$m, $Z_R = 1.083$ cm, and $\kappa = 2.74331$.

A comparison of the transverse profiles of the initial (red) and filtered (black) pulses can be seen in Fig. 8(c). In addition to filtering, the sharp cutoff of the filter leads to strong internal reflection and mode excitation, which means that even for a perfect, Gaussian pulse on entry, there will be modest but noticeable generation of higher-order modes. This can be seen in the transverse profile of the filtered pulse, where it has small but long lived wings. Likewise, the sharp truncation requires significantly long filters, on the order of 20 cm, before filtering out the initial higher-order mode content. This is challenging in present experiments, as experimentally-demonstrated gas jet generated leaky channels are thus far at most 5–7 centimeters in length by concatenating several such jets. However, if one was to use a discharge capillary that was designed and prepared for energy to be leaked out, then such long, sharply truncated leaky channels could be realized.

A solution to mode excitation and slow filtering of the truncated channel is to use a channel that is tailored to leak out higher-order modes faster, as well as not generate them as strongly. A simple analytical candidate for this is an exponentially decaying parabolic channel, which comes about naturally in the earlier evolution of a hydroshock generated channel, which is visualized in Fig. 3. This can be seen in Fig. 9(a), where a parabolic channel with exponentially decaying walls is used to guide a laser pulse (red). Once again, we compare it to a pulse injected directly into a matched parabolic channel (black), and we can see the stark difference in terms of mismatched guiding. The laser energy depletion is similar to that of a sharp truncation. We are using the same numerical parameters as in the sharply truncated channel, except now the filter length is 6.5 cm = 6 Z_R and is characterized by $k_{p0}r_{\mathrm{ED}} = 3.86$ and a slight channel mismatching with $R = 0.856r_0$.

It has been found that leaky channels with steeper walls, i.e., smaller than matched channel radii, e.g., $R_{\mathrm{eff}} = 27\ \mu$m for $r_0 = 53\ \mu$m, where R_{eff} comes from the Taylor-expansion of $n(r)$ as seen in Eq. (3), both guide the main lobe and leak out higher-order modes more efficiently. In this case, however, the effective radius approximates a mismatched plasma channel, which here causes the pulse to focus. When $R_{\mathrm{eff}} < r_0$, we get greater leakage rates of all modes, which leads to a faster filtering of the injected pulse, although steep density profiles are more difficult to practically achieve in experiment.

In Fig. 9(b), it appears that only a marginal amount of higher-order mode content is leaked out. However, this modal decomposition is done for the laser intensity and so does not account for a change in sign in the individual mode coefficients, which in turn minimizes the presence of sidelobes. Once again, we see that the sidelobes, i.e., the higher-order modes, are minimized when we compare the initial transverse pulse profile to that of a filtered pulse, of Fig. 9(c). An important advantage of the exponentially decaying leaky channel is that the simulated plasma filter is only several centimeters in length, which has a notably faster filtering in comparison to the sharply truncated leaky channel. This is likely due to two factors: the effectively thicker wall of the exponentially decaying channel reduces the leakage rate of confined modes, but the negative density gradient outside the channel effectively acts as a diffracting lens for the laser content that has already leaked out.

VI. SUMMARY AND CONCLUSIONS

In this paper, we have investigated the application of leaky channels to mode filtering non-Gaussian laser pulses for potential use in LPAs. Realistic, experimental pulses are super-Gaussian after pumping and focus down to a near jinc profile with the sidelobes at focus. A jinc type pulse, which can be expressed as a superposition of LG modes, leads to mode beating and in turn to poor guiding, which can lead to

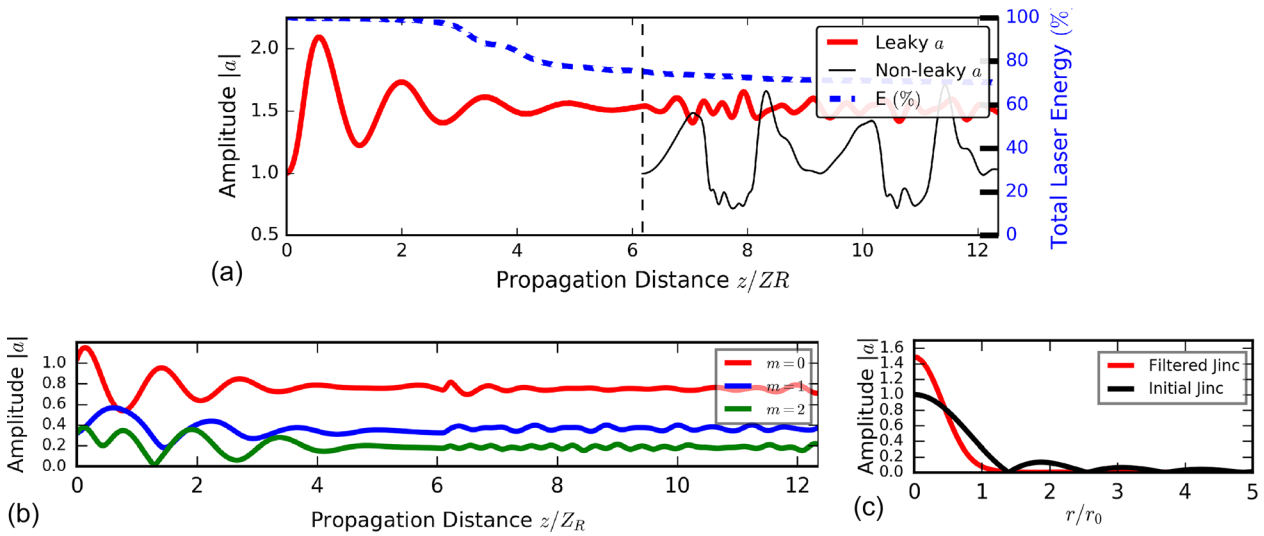

FIG. 9. An exponentially decaying leaky channel ($k_{p0}r_{\mathrm{ED}} = 3.86$, $R = 0.856r_0$, $n_{\mathrm{filter}} = 10^{17}$ cm^{-3}, and length of 6.5 cm), acting as a filter, precedes a parabolic capillary discharge channel with $n_0 = 3 \times 10^{17}$ cm^{-3} and $R = 30\ \mu$m. (a) The laser amplitude propagating through the filter into a parabolic channel (red), an unfiltered jinc pulse propagating just through an approximately matched infinite channel (black), and the energy content of the filtered pulse (blue). (b) Modal decomposition of intensity. The color lines represent the fundamental (red), 1st (blue), and 2nd (green) higher-order modes on the basis of an LG decomposition. (c) The initial, unfiltered pulse profile (black) and filtered pulse profile (red), where $a_\perp(0) = 0.5$, $r_0 = 53\ \mu$m, $Z_R = 1.083$ cm, and $\kappa = 2.74331$.

electron bunch loss in a laser-plasma accelerator. We have demonstrated using the WKB method that we can accurately calculate the leakage rate of LG modes. Likewise, we can couple the WKB result via a leakage coefficient to the SDE formalism that allows for us to accurately model the evolution of multi-mode LG pulses in leaky channels. The accuracy of the SDE method was verified by comparisons to full PIC simulations. Numerically, we investigated both a sharply truncated as well as exponentially decaying channels. Both are able to filter out higher-order modes, but the latter is able to do so more rapidly, especially when mismatched. The two forms of leaky channels tested are based on laser-ignited hydrodynamic shock expansion at different points of the plasma channel evolution.

Implementation of leaky channel plasma structures and potentially mode transforming filters to generate single-mode Gaussian pulses have the potential to greatly improve future LPA experiments that rely on laser guiding in parabolic plasma channels. Two specific examples were examined in which a leaky channel was placed immediately in front of an idealized parabolic channel in order to improve guiding (reduce mismatch, spot size oscillations, and improve pulse evolution) in the parabolic channel. In the first case, a 16 cm long leaky channel with a sharp truncation was used. Matching in the parabolic channel was greatly improved due to the preferential loss in power for the higher order modes compared to the fundamental Gaussian in the leaky channel. Approximately 75% of the initial laser power was coupled into the parabolic channel in a near-matched mode. In the second case, a 7 cm-long leaky channel with exponential truncation was used. Matching into the parabolic channel was improved due to a rephasing of the higher-order modes in the leaky channel. Over 70% of the initial laser power was coupled into the parabolic channel in a near-matched mode. This improvement in matched propagation will greatly improve the performance of laser-plasma accelerators.

In prior experimental work, leaky channels have been produced in gas jet plasmas with lengths on the order of a few centimeters. Longer channels may be created in capillary discharges using laser-assisted heating.[29] A secondary problem not considered in this work is the potential damage by and containment of this leaked energy, as several Joules of laser energy (for a GeV LPA) would be leaked into the walls of a capillary based structure. Another possibility is to incorporate a gas jet earlier in the chirped pulse amplification process altogether. Placing a leaky channel immediately after the power amplifiers, where the flat-top profile originates and a higher order mode content is primarily introduced, but before compression, can take advantage of the long pulse, low fluence properties of the laser pulse at this point. Here, the laser pulse can be focused to a very small spot size, thereby, shortening the Rayleigh length and so the length of the filter, while also allowing one to completely neglect plasma wake effects. This would have the advantage that the filtered pulse would then put a lesser strain on the compression gratings used in the amplification process, as well as resulting in a more Gaussian pulse in the end. However, the effect of long-pulse laser-plasma instabilities (e.g., Raman backward scattering) during uncompressed-laser propagation would need further investigation.

ACKNOWLEDGMENTS

The authors acknowledge contributions from members of the BELLA Program at the Lawrence Berkeley National Laboratory. This work was supported by the Director, Office of Science, Office of High Energy Physics, of the U.S. Department of Energy under Contract No. DE-AC02-05CH11231, as well as by the NSF through Grant No. PHY-1632796.

[1]M. Tabak, J. Hammer, M. E. Glinsky, W. L. Kruer, S. C. Wilks, J. Woodworth, E. M. Campbell, M. D. Perry, and R. J. Mason, Phys. Plasmas **1**, 1626 (1994).
[2]H. M. Milchberg, C. G. Durfee II, and T. J. McIlrath, Phys. Rev. Lett. **75**, 2494 (1995).
[3]D. C. Eder, P. Amendt, L. B. DaSilva, R. A. London, B. J. MacGowan, D. L. Matthaws, B. M. Penetrante, M. D. Rosen, S. C. Wilks, T. D. Donnelly, R. W. Falcone, and G. L. Strobel, Phys. Plasmas **1**, 1744 (1994).
[4]E. Esarey, C. B. Schroeder, and W. P. Leemans, Rev. Mod. Phys. **81**, 1229 (2009).
[5]W. P. Leemans, A. J. Gonsalves, H.-S. Mao, K. Nakamura, C. Benedetti, C. B. Schroeder, C. Toth, J. Daniels, D. E. Mittelberger, S. S. Bulanov, J.-L. Vay, C. G. R. Geddes, and E. Esarey, Phys. Rev. Lett. **113**, 245002 (2014).
[6]A. J. Gonsalves, K. Nakamura, J. Daniels, H.-S. Mao, C. Benedetti, C. B. Schroeder, C. Tóth, J. van Tilborg, D. E. Mittelberger, S. S. Bulanov, J.-L. Vay, C. G. R. Geddes, E. Esarey, and W. P. Leemans, Phys. Plasmas **22**, 056703 (2015).
[7]C. Benedetti, F. Rossi, C. B. Schroeder, E. Esarey, and W. P. Leemans, Phys. Rev. E **92**, 023109 (2015).
[8]I. Gris-Sánchez, D. Van Ras, and T. A. Birks, Optica **3**, 270 (2016).
[9]A. J. Gonsalves, private Communication (2017).
[10]H. M. Milchberg, K. Y. Kim, V. Kumarappan, B. D. Layer, and H. Sheng, Phys. Trans. R. Soc. **364**, 647–661 (2006).
[11]C. Durfee and H. M. Milchberg, Phys. Rev. E **51**, 2368–2396 (1995).
[12]P. Volfbeyn, E. Esarey, and W. P. Leemans, Phys. Plasmas **6**, 2269–2277 (1999).
[13]T. Antonsen and P. Mora, Phys. Rev. Lett. **72**, 4440–4443 (1995).
[14]P. Sprangle, A. Ting, and C. M. Tang, Phys. Rev. A **36**, 2773–2781 (1987).
[15]P. Sprangle, E. Esarey, and J. Krall, Phys. Rev. E **54**, 4211–4232 (1996).
[16]E. Esarey and W. P. Leemans, Phys. Rev. E **59**, 1082–1095 (1999).
[17]P. Sprangle, B. Hafizi, and J. R. Peñano, Phys. Rev. E **61**, 4381 (2000).
[18]A. H. Hartog and M. J. Adams, Opt. Quantum Electron. **9**, 223–232 (1977).
[19]J. P. Palastro, T. M. Antonsen, S. Morshed, A. G. York, and H. M. Milchberg, Phys. Rev. E **77**, 036405 (2008).
[20]C. Benedetti, C. B. Schroeder, E. Esarey, C. G. R. Geddes, and W. P. Leemans, AIP Conf. Proc. **1299**, 250–255 (2010).
[21]C. Benedetti, C. B. Schroeder, C. G. R. Geddes, E. Esarey, and W. P. Leemans, Plasma Phys. Controlled Fusion **60**, 014002 (2018).
[22]E. Cormier-Michel, E. Esarey, C. G. R. Geddes, C. B. Schroeder, K. Paul, P. J. Mullowney, J. R. Cary, and W. P. Leemans, Phys. Rev. Accel. Beams **14**, 031303 (2011).
[23]C. Ren, B. J. Duda, R. G. Hemker, W. B. Mori, T. Katsouleas, Jr., and T. M. Antonsen, Phys. Rev. E **63**, 026411 (2001).
[24]J. P. Palastro, D. Gordon, B. Hafizi, L. A. Johnson, J. Peñano, R. F. Hubbard, M. Helle, and D. Kaganovich, Phys. Plasmas **22**, 123101 (2015).
[25]A. Snyder and J. Love, *Optical Waveguide Theory* (Chapman and Hall, New York, 1983).
[26]L. Brekhovskikh, *Waves in Layered Media* (Academic Press, New York, 1960).
[27]S. Golowich, W. White, and W. A. Reed, J. Lightwave Technol. **21**, 111–121 (2003).
[28]E. Esarey, P. Sprangle, J. Krall, and A. Ting, IEEE J. Quantum Electron. **33**, 1879 (1997).
[29]N. A. Bobrova, P. V. Sasorov, and C. Benedetti, Phys. Plasmas **20**, 020703 (2013).